



Published in final edited form as:

J Cardiovasc Electrophysiol. 2015 October ; 26(10): 1117–1126. doi:10.1111/jce.12753.

Modifying Ventricular Fibrillation by Targeted Rotor Substrate Ablation: Proof-of-Concept from Experimental Studies to Clinical VF

DAVID E. KRUMMEN, M.D., F.H.R.S.^{*,†}, JUSTIN HAYASE, M.D.^{*,†}, STEPHEN P. VAMPOLA, M.D.^{*,†}, GORDON HO, M.D.^{*,†}, AMIR A. SCHRICKER, M.D.^{*,†}, GAUTAM G. LALANI, M.D.^{*,†}, TINA BAYKANER, M.D.^{*,†}, TAYLOR M. COE, B.S.[‡], PAUL CLOPTON, M.S.[†], WOUTER-JAN RAPPEL, Ph.d.[§], JEFFREY H. OMENS, Ph.d.[‡], and SANJIV M. NARAYAN, M.D., Ph.d., F.H.R.S.[¶]

^{*}Department of Medicine, University of California, San Diego, California, USA

[†]Veterans Affairs San Diego Healthcare System, San Diego, California, USA

[‡]Department of Bioengineering, University of California, San Diego, California, USA

[§]Department of Physics, University of California, San Diego, California, USA

[¶]Stanford University, Palo Alto, California, USA

Abstract

Introduction—Recent work has suggested a role for organized sources in sustaining ventricular fibrillation (VF). We assessed whether ablation of rotor substrate could modulate VF inducibility in canines, and used this proof-of-concept as a foundation to suppress antiarrhythmic drug-refractory clinical VF in a patient with structural heart disease.

Methods and Results—In 9 dogs, we introduced 64-electrode basket catheters into one or both ventricles, used rapid pacing at a recorded induction threshold to initiate VF, and then defibrillated after 18 ± 8 seconds. Endocardial rotor sites were identified from basket recordings using phase mapping, and ablation was performed at nonrotor (sham) locations (7 ± 2 minutes) and then at rotor sites (8 ± 2 minutes, $P = 0.10$ vs. sham); the induction threshold was remeasured after each. Sham ablation did not alter canine VF induction threshold (preablation 150 ± 16 milliseconds, postablation 144 ± 16 milliseconds, $P = 0.54$). However, rotor site ablation rendered VF noninducible in 6/9 animals ($P = 0.041$), and increased VF induction threshold in the remaining 3. Clinical proof-of-concept was performed in a patient with repetitive ICD shocks due to VF refractory to antiarrhythmic drugs. Following biventricular basket insertion, VF was induced and

Address for correspondence: David E. Krummen, M.D., 3350 La Jolla Village Drive, Cardiology Section 111A, San Diego CA, 92161, USA. Fax: 858-552-7490; dkrummen@ucsd.edu.

Other authors: No disclosures.

Dr. Krummen has served as a consultant to Topera Inc., and has received fellowship program support from Medtronic, Boston Scientific, St. Jude, Biotronik, and Biosense-Webster. Dr. Omens has served as a consultant to InsilicoMed. Drs. Rappel and Narayan are co-inventors on intellectual property owned by the University of California and licensed to Topera, Inc. Dr. Narayan is a consultant to InsilicoMed, Abbott Electrophysiology and Medtronic.

Supporting Information

Additional supporting information may be found in the online version of this article at the publisher's website:

then defibrillated. Mapping identified 4 rotors localized at borderzone tissue, and rotor site ablation (6.3 ± 1.5 minutes/site) rendered VF noninducible. The VF burden fell from 7 ICD shocks in 8 months preablation to zero ICD therapies at 1 year, without antiarrhythmic medications.

Conclusions—Targeted rotor substrate ablation suppressed VF in an experimental model and a patient with refractory VF. Further studies are warranted on the efficacy of VF source modulation.

Keywords

catheter ablation; implantable cardioverter defibrillator; phase mapping; rotors; ventricular fibrillation

Introduction

Ventricular fibrillation (VF) remains an important public health problem, accounting for significant morbidity and mortality.¹ The implantable cardioverter-defibrillator (ICD) is the cornerstone of current therapy for this life-threatening arrhythmia, applied either in high-risk patients² or VF-survivors.³ While effective, defibrillation results in anxiety, depression,⁴ and increases the risk of death in patients receiving such therapy.⁵

Currently, therapies to prevent VF are limited. Antiarrhythmic drugs have limited efficacy,⁶ and may result in serious adverse events.⁷ Ablation strategies have been devised for patients with monomorphic PVC triggers or channelopathy-related ventricular arrhythmias^{8,9} in whom ablation of triggers from the His–Purkinje system,¹⁰ outflow tracts, and papillary muscles¹¹ can suppress VF. However, an incomplete understanding of perpetuating mechanisms has impeded the routine use of ablation in clinical VF for patients without such characteristics.

To date, electrical spiral waves (rotors) have been observed on the endocardium and epicardium in animal¹² and human^{13–15} studies of VF, and may exhibit spatial conservation over repeated VF inductions.¹⁵ Attempts to alter VF have been performed in a canine model,¹⁶ but whether this concept could be translated to treat human VF as has been shown in atrial fibrillation¹⁷ remains untested. We hypothesized that if VF is sustained by conserved rotors detectable on the endocardium, targeted ablation at such substrate may modulate subsequent initiation of sustained VF. In a feasibility study we tested the impact of VF rotor modulation in an animal model. Since animal studies were promising, we translated this approach to perform directed human VF rotor site ablation in a patient with structural disease and VF refractory to standard antiarrhythmic medications.

Methods

Animal studies were performed according to the National Institutes of Health Guide for the Care and Use of Laboratory Animals. Experimental protocols were approved by the Animal Subjects Committee of the University of California, San Diego, which is accredited by the American Association for Accreditation of Laboratory Animal Care.

Clinical studies were performed under a specific Institutional Review Board (UCSD and VA San Diego)-approved protocol (clinicaltrials.gov: NCT01492764). The patient presented

with multiple, drug-refractory ICD shocks for VF. Written informed consent was obtained after full discussion risks and potential benefits of the approach.

Canine Procedural Protocol

Adult mongrel dogs (age 2.5 ± 2 years, weight 20 ± 3 kg) were premedicated with acepromazine (0.05 mg/kg) and morphine (0.5 mg/kg), sedated with a single administration of propofol (4–6 mg/kg dose), and mechanically ventilated with isoflurane (1.5–2.5%). Sheaths were placed in both femoral arteries and veins via cutdown, and a steerable decapolar catheter (Polaris, Boston Scientific, Natick, MA, USA) was advanced into the RV apex under fluoroscopic guidance for ventricular pacing.

A 64-electrode basket catheter (Constellation, Boston Scientific) was introduced into the LV via the retrograde aortic route in all dogs, and simultaneously in both ventricles in $n = 3$ (Fig. 1A). Basket catheter electrograms were recorded as bipolar signals during sinus rhythm (Fig. 1B and Online Supporting Fig. S1A), and then as unipolar signals during the rapid pacing protocol for VF initiation (Fig. 1C), and observed ventricular activation was validated against expected patterns.^{18,19} Signals were filtered between 0.05 and 500 Hz (20) with 16-bit resolution at 1000 Hz (Bard Pro, Boston Scientific, USA).

VF was induced with programmed stimulation consisting of triple extrastimulus pacing then burst pacing at twice diastolic threshold from the right ventricle using a stimulator (Medtronic 5328, Minneapolis, MN, USA). Rapid pacing consisted of 5 seconds at a cycle length (CL) of 300 milliseconds, decreasing in 20 milliseconds steps until a CL of 200 milliseconds was reached, after which the CL was decreased in 10 milliseconds increments until VF was induced (Fig. 1D) or 2:1 capture was observed, analogous to prior work.²⁰ VF was allowed to continue for 10 seconds for mapping, after which the external defibrillator was charged to 200 J and the animal defibrillated externally, similar to clinical descriptions.²¹ The VF threshold (VFT) was defined as the longest pacing cycle length able to induce VF.²⁰

Mapping

Multipolar basket electrograms were analyzed offline using RhythmView (Topera Inc., Menlo Park, CA, USA) as described previously,²² using phase analysis²³ of unipolar electrograms (Fig. 2A),¹⁴ within physiologic constraints.^{24,25} Data were analyzed for the first 10 seconds of VF or until VF terminated, whichever came first.

Rotational activity was identified as a phase singularity formed at the intersection of depolarization and repolarization isolines.²⁶ Rotors (Fig. 2B) were defined as regions of rotational activity that controlled surrounding activation.¹² Centrifugal propagation (Fig. 2C) without rotation was defined as focal activity.¹⁵ Disorganized activation¹⁵ without clear rotational or focal activity (Fig. 2D) was also documented.

We quantified the prevalence of rotational activity as the percent of VF cycles showing such activity, and stability as the maximum number of consecutive revolutions of electrical activity within a region bounded by 2 electrodes in each axis.¹⁵ Additionally, we cross-referenced rotor sites from analysis of phase maps from unipolar recordings with the bipolar

recordings obtained during sinus rhythm to evaluate for the prevalence of Purkinje activity at rotor sites (Online Supplement, Section II and Fig. S1A).

Canine Sham (Nonrotor) and Rotor Substrate Ablation

Control (nonrotor, “sham”) and rotor substrate site ablation were performed using each animal as their own control. Sham ablation was performed >3 cm from any identified rotor site, using an 8-mm ablation catheter (EPT, Boston Scientific, Natick, MA, USA) at 55 W, 55 °C for 30–60 seconds per location, for 5–10 minutes of energy delivery per site. Ablation¹¹ had a goal ablation area of approximately 1.5–2.0 cm².

Following sham ablation, VF induction was performed to determine VF threshold using the study pacing protocol until VF induction or 2:1 capture. If VF was induced, the defibrillator was charged and the animal was defibrillated. The animal was allowed to recover for at least 5 minutes before subsequent ablation.

Next, VF rotor substrate ablation was performed, targeting observed rotor sites referenced to basket splines (A–H) and electrodes (1–8) visualized with fluoroscopy.²² Ablation was performed in the same manner as sham ablation. Following rotor site ablation, VF threshold was again measured and, if VF was induced, mapping was performed again as described.

In 1 animal, the order of ablation was reversed so that rotor ablation was performed prior to sham in order to evaluate whether observed effects of rotor ablation were confounded by the cumulative effect of sham plus rotor ablation.

Electrograms were carefully analyzed to evaluate Purkinje activity at sham and rotor sites; Purkinje potentials were defined per prior work.²⁷ At the conclusion of the protocol, animals were sacrificed using pentobarbital sodium and examination of ablation lesions was performed.

Human Procedural Protocol

The enrolled patient was a 72-year-old male with ischemic cardiomyopathy with history of prior coronary artery bypass graft surgery and multiple percutaneous coronary interventions. Ejection fraction was 21% with NYHA class III symptoms, and he had undergone ICD implant, upgraded to biventricular ICD in the prior year. He had previously been intolerant of amiodarone (severe skin rash), and his VF was refractory to sotalol; he had experienced 7 ICD shocks in the 8 months prior to this procedure, with 5 shocks being in the last 3 months despite increasing doses of sotalol. His ICD was programmed with VT zone at 170 bpm with therapies: ATPx4, 36Jx1, 41Jx5. VF zone was programmed at 200 bpm with therapies: ATPx1, 36Jx1, 41Jx7.

For the procedure, the patient was placed under general anesthesia. Coronary sinus and right ventricular catheters were positioned. Voltage maps (NavX, St. Jude Medical) were created of both ventricles using a 3.5 mm open-irrigated catheter (Thermocool, Biosense-Webster, Diamond Bar, CA, USA). Basket catheters were advanced into the left ventricle (transseptally) and right ventricle simultaneously, and an electrophysiology study was

performed analogous to the animal study to induce VF. This comprised single, double and triple ventricular extrastimuli, from the LV.

Defibrillator charging was initiated as soon as VF was induced, and VF was recorded in the interval up to defibrillation.¹⁵ Biventricular VF maps were analyzed for the period of VF prior to defibrillation.

Human Rotor Substrate Ablation

Identified endocardial rotor sites were targeted for ablation. Ablation was performed at 35 W and targeted a 12-ohm impedance drop.¹¹ Following ablation, we retested VF inducibility. The presence of Purkinje potentials at ablation sites was carefully evaluated as described for canine ablation (Online Supplement, Section II, Fig. S1B). After the procedure, ICD settings were unchanged and no antiarrhythmic drugs were prescribed. The patient was followed carefully by ICD interrogation at monthly intervals, with interim telephone follow-up to identify any incipient adverse events including pro-arrhythmia.

Statistical Methods

Continuous variables were expressed as mean \pm standard deviation. The paired *t*-test was used to evaluate changes in VF induction threshold. Repeated measures analysis-of-variance with post hoc Bonferroni was used to compare the proportion of VF cycles with rotors, focal sources, and disorganized activation. The McNemar test was used to compare inducibility in sham versus targeted ablation. Subject-wise and episode-wise statistics are indicated. Statistics were calculated using SPSS 19 (IBM, Somers, NY, USA).

Results

Canine VF

Voltage mapping in the canine model revealed preserved voltages throughout both ventricles. Triple extrastimulus pacing did not induce VF in canines; sustained VF (CL 121 ± 13 milliseconds) was induced in all study animals (Table 1) with 5 seconds of rapid pacing at a cycle length of 150 ± 16 milliseconds. Canine VF was predominantly characterized by LV rotors ($56 \pm 14\%$ of VF cycles, see online supporting Movie S1), with smaller proportions of disorganized activity ($35 \pm 15\%$ of cycles, $P = 0.01$), and focal activation ($7 \pm 11\%$ of cycles, $P < 0.001$, Fig. 2E); RV rotors were rare and unstable, and thus not consistent with drivers. On average, 1.3 ± 0.5 [range 1–2] endocardial rotors were observed, with an average maximum stability of 10.9 ± 4.1 [range 7–19] rotations (Fig. 2F) persisting 1.33 ± 0.50 seconds.

Canine Nonrotor (Sham) and Rotor Substrate Ablation

Sham ablation ($n = 9$ canines, see Online Appendix, Section III for additional details) involved 6.7 ± 2.2 minutes of RF delivery over areas of 1.6 ± 0.2 cm². Sham ablation had no appreciable effect on the VF induction threshold: pacing CL required to induce VF was 144 ± 16 milliseconds following nonrotor site ablation (vs. preablation 150 ± 16 , $P = 0.54$; Online Appendix Fig. S2 illustrates sham ablation and subsequent VF induction threshold testing).

Targeted rotor substrate ablation rendered VF noninducible in 6 of 9 animals ($P = 0.041$ for noninducibility). In the remaining animals, VF was reinducible at a higher induction threshold (faster pacing CL of 128 ± 16 milliseconds) versus preablation (156 ± 14 milliseconds, $P = 0.002$). There was no difference in maximum rotor stability in these subjects pre- and postablation (12.7 ± 4.2 preablation versus 8 ± 5.6 rotations postablation, $P = 0.21$). Sham and rotor substrate ablation lesions exhibited epicardial or contralateral septal discoloration/edema, consistent with transmural lesions.

Figure 3 shows a canine in which sustained VF was initiated with rapid pacing at a CL of 130 milliseconds preablation (Fig. 3A). A rotor was observed at the posteroseptal LV (Fig. 3B). Sham ablation was performed and VF was reinducible with rapid pacing at a CL of 130 milliseconds. Following targeted rotor site ablation (shown in Fig. 3C), sustained VF could not be initiated with the pacing protocol (Fig. 3D). Figure 3E shows the proportion of VF patterns prerotor site ablation (red bars) and postrotor site ablation (blue bars); indicating the lower proportion of rotors during the brief, nonsustained episode of VF after ablation. Figure 3F shows gross pathological specimen of a targeted rotor site ablation (green arrow), with an area of 2.2 cm^2 .

For the animal in which the order of ablation was reversed, VF induction threshold increased 19% (required pacing cycle length decreased from 160 to 130 milliseconds), after VF rotor site ablation. Sham ablation was then performed, with no change in VF threshold (130 milliseconds).

In canines, high-frequency signals consistent with Purkinje potentials were rare, observed at similar proportions of sham ($6 \pm 11\%$) and VF rotor substrate sites ($9 \pm 14\%$, $P = 0.54$).

Human VF Rotor Site Ablation and Follow-up

Clinical VF from remote monitoring is shown in Figure 4A. The patient's increasing burden of ICD shocks for VF prior to electrophysiology study is shown in Figure 4B. ICD interrogation prior to the procedure revealed that 3 or more different PVC origins initiated sustained VF (and nonsustained arrhythmias, online supplement Section IV): 2 distinct morphologies closer to the LV lead (Fig. 4C,D) and a third closer to the RV lead (Fig. 4E) which elicited triggered LV pacing.

At electrophysiology study, rare, multifocal PVCs were observed at baseline. Following biventricular basket insertion (Fig. 5A), triple extrastimulus pacing at 500–330–240–180 milliseconds initiated sustained VF (CL 213 milliseconds, Fig. 5B and 5C). VF phase analysis of recorded electro-grams (Fig. 5C) revealed 4 rotors: 2 LV (Fig. 5D and online supporting Movie S2) and 2 RV (Fig. 5E, F), located at the mid-lateral and mid-inferior LV, and the anterolateral and posterior RV.

Rotor sites were targeted for ablation (Fig. 6A), delivering 6.3 ± 1.5 minutes of RF energy to each site. The LV rotors were located at the borderzone tissue adjacent to a large inferolateral scar (Fig. 6B), and the RV rotors were located at borderzone tissue at the mid-antrolateral and basal posterior aspects of the RV (Fig. 6C). High-frequency signals consistent with Purkinje potentials were rare at rotor substrate sites, observed at 3 of 27

ablation lesions (11%), none at LV rotor site 1 or RV rotor site 2. The anterolateral RV rotor substrate site was approximately 1 cm from the anterior papillary muscle; other rotor substrate sites were not adjacent (< 2 cm) to papillary muscles. No other endocardial structures were observed at the rotor substrate sites using intracardiac echocardiography.

Following ablation (white ablation lesions, Fig. 6B, C), triple extrastimulus pacing at 500–320–220–190 milliseconds induced 5 cycles of self-limiting ventricular fibrillation (cycle length 245 milliseconds; Fig. 6D) but did not induce sustained VF. Notably, the activation pattern for this nonsustained ventricular arrhythmia was substantially altered compared with preablation (Fig. 6E), similar to the animal study, with a reduction in the prevalence of rotors (51–0%). Sustained VF was no longer inducible with triple extrastimulus pacing. The patient has consistently been seen at 3-month intervals postablation. There has been no significant change in his ejection fraction as measured by echocardiography both at 1 month and 1 year (EF 23%) postprocedure. Importantly, he has had no sustained VF events and zero ICD therapies in the 1 year since the rotor site ablation procedure (Fig. 6F).

Discussion

There are 2 major findings in the present study. First, ablation at detected endocardial VF rotor substrate in a canine model decreased VF inducibility, while ablation distant from rotor substrate had no impact. Second, targeted VF rotor substrate ablation alone in a patient with previously antiarrhythmic-refractory VF completely eliminated VF over a 1-year follow-up without antiarrhythmic drugs. These findings support the hypothesis that electrical rotors contribute to the mechanisms maintaining VF, and that ablation of rotor sites may prevent sustained VF.

The Role of Ventricular Fibrillation Rotors

Increasing numbers of studies support rotors as a sustaining mechanism for cardiac fibrillation. First observed in a sheep model of VF,²⁸ they have been reported in humans using high-density epicardial electrode arrays.¹⁴ Studies of VF rate gradients in an ischemia model of VF²⁹ and recent work from our laboratory demonstrate that VF rotors exhibit clear spatial preferences and are conserved across repeated inductions of VF.¹⁵ Such spatial homogeneity reflects a dependence upon functional³⁰ and structural alterations,¹³ which promote their formation and stabilization. Such stabilization has been shown to predict VF outcome,¹⁵ but this relationship had not previously been supported by rotor site modulation via ablation and attempted arrhythmia re-induction in humans.

An increasing body of work suggests that rotor ablation prevents subsequent fibrillation. The CONFIRM trial¹⁷ and later independent work³¹ showed that AF rotor ablation improves procedural outcome at both intermediate and long-term³² follow-up. In prior work, ablation was shown to suppress canine VF;¹⁶ however, ablation was anatomically rather than functionally guided. Furthermore, ablation was extensive both in duration (~60 minutes) and spatial distribution (basal to apical LV), and therefore less suitable for routine clinical usage.

Similar to prior work, VF rotor substrate ablation in this study was performed during sinus rhythm. Because of this, the direct effects of ablation on scroll waves are unclear. Instead,

our data support the hypothesis that modulation of rotor substrate sites inhibits the formation and stabilization of rotors (scroll waves), and thus increases the VF induction threshold, rather than directly affecting rotors (scroll waves) themselves. Future work is required to determine the effect of ablation during ongoing VF.

Insights from Canine Studies

Our animal studies show that rotor substrate ablation is feasible and may reduce susceptibility to VF. There was a similar prevalence of rotors in this study ($56 \pm 14\%$) compared to what has been seen in humans.¹⁵ From a safety perspective, neither rotor site nor sham ablation produced substrate leading to refractory VF in structurally normal ventricles. We also found that ablation at 1–2 canine VF rotor substrate sites prevented VF induction using the pacing protocol in most animals, and increased the VF induction thresholds in the others, without requiring the more extensive ablation performed in prior work.¹⁶ Sham ablation had no effect on the VF induction threshold, whether performed before or after rotor site ablation.

Human Study Findings

Prior work has shown that human VF is similar between pacing and shock-induced episodes,^{15,33} suggesting that clinical VF may exhibit conserved mechanisms with VF induced at electrophysiology study. Based on the success of the animal study results, we proceeded with the first human targeted VF rotor site ablation, which was effective in suppressing recurrent episodes in a patient with clinical VF refractory to antiarrhythmic medications. Notably, RV and LV rotors localized to borderzone tissue, consistent with prior work.¹³

Interestingly, following ablation of rotor substrate sites alone, only self-limited VF could be induced despite similarly aggressive induction attempts of protocol-driven²⁰ pacing.¹⁵ The activation pattern of this nonsustained VF was markedly different than preablation, with little rotor activity. This change mirrors the reduction in rotor stability seen in canines following VF rotor site ablation. These data reinforce the findings of prior work showing the importance of the initiation and stabilization of rotors to VF perpetuation.¹⁵

Relationship to Other Work

Prior work in VF ablation has focused on ablation of VF triggers from Purkinje fibers,^{8,10} outflow tracts, and papillary muscles,¹¹ whose ablation decreased VF events. However, the utility of this approach in patients with rare, polymorphic PVCs and substantial structural disease, as seen in this patient, which may lie at sites remote from the Purkinje system or other identifiable anatomical sites, is unclear. In our study, rotors were infrequently located at Purkinje sites; further work is required to determine the precise relationship between rotors and Purkinje fibers.

Importantly, our findings directly implicate rotors as a perpetuating mechanism of VF, as previously suggested by animal work,³⁴ human observations,¹³ and computational studies.³⁵ Larger studies of VF rotor substrate modulation via ablation are required to evaluate the

broader applicability of this technique. Future studies should also examine the precise functional and anatomic abnormalities which support rotor formation in susceptible patients.

Limitations

A limitation of this study is the fact that the canine model of VF lacked ischemic cardiomyopathy, which was present in our patient, and thus the relationship between the 2 substrates for VF is indirect. However, the canine model and human were linked by the presence of inducible, sustained VF, with similarities in observed endocardial rotors. Because localized ablation was able to alter VF inducibility in both groups, it suggests that spatially conserved rotor sites are mechanistically central to sustaining VF, and not exclusive to a particular substrate or disease process. If confirmed in larger trials, our ablation approach may form the basis for a new therapeutic approach in the management of clinical VF. A second limitation involves the spatial resolution of the LV and RV 64-electrode basket catheters (4–5 mm inter-electrode, ~10 mm interspline). Such resolution may miss activation patterns around and within more complex anatomical geometry such as the papillary muscles, and may be suboptimally positioned to record Purkinje potentials at the rotor core. However, the resolution was sufficient to “triangulate” rotor substrate locations between adjacent electrodes, and allowed ablation to impact VF inducibility. Importantly, unmapped regions are consistent in the same subject, making interepisode epochs comparable.³⁶ Future studies are required to better define the optimal extent of mapping and ablation required to inhibit VF. Third, only the endocardium was mapped. Endocardial mapping may misclassify nonendocardial rotors as focal sources, and thus underestimate the true prevalence of VF rotors. However, only a minority of mapped focal sources were consistent with rotors, placing an upper limit (<10–20%)¹⁵ on this possibility. Fourth, for practical reasons we could study only the first few seconds of VF. Early VF is critical, however, because it initiates the cascade of events leading to sustained VF and clinical sequelae. Fifth, we studied only a small number of animals and a single patient, though we have reported a case³⁷ in which rotor ablation serendipitously occurred, and VF was subsequently not inducible, and clinical VF was suppressed. Sixth, for safety reasons, sham ablation was not carried out in our patient, as it was in canines. Seventh, it is possible that not all lesions were transmural, since average left ventricular thickness for canines in this study was 0.8 ± 0.1 cm.³⁸ Since clinical endocardial VT ablation can frequently be successful³⁹ even if lesions are not transmural, it is possible that critical VF-maintaining substrates were not epicardial in our study, consistent with papillary and other endocardial locations reported previously.³⁰ Eighth, canines received a single dose of propofol for initial sedation, which may have altered the electrophysiological properties of the heart and affected rotor formation and characteristics. Future studies with alternative sedating agents should be considered to avoid the potential confounding effect of propofol. Finally, it is possible that ablation of an alternative mechanism, such as Purkinje fibers, and not VF rotor sites, is responsible for the clinical effects seen in this study. However, the low prevalence of Purkinje potentials at VF rotor substrate ablation sites ($9 \pm 14\%$ in canines, 11% in the human case) makes this scenario unlikely.

Conclusions

Ablation of rotor sites decreases susceptibility to VF in an animal model. As a proof-of-concept, we then performed VF rotor site ablation alone in a patient with VF refractory to antiarrhythmic therapy, which eliminated further episodes of VF without the need for antiarrhythmic medications. Further studies are needed to define the safety and efficacy of rotor site ablation for VF management, and to determine the precise structural and functional abnormalities which promote VF rotor formation.

Supplementary Material

Refer to Web version on PubMed Central for supplementary material.

Acknowledgments

We would like to thank Mohammad Sedarat, BS, Diane Huang, BS, Jonathan Barboza, BS, Helen Leung, BS, Brianna Potter, BS, Ayla Sessions, BS, Tanaya Pattnaik, BS, Ryan Smith, BS, Hugo Aguilar, BS, Andy Edwards, PhD, Alejandro Vargas, BS, Katrina Go, PhD for their assistance with the canine study. We are indebted to Kathleen Mills, BA for coordinating the clinical study. We also wish to thank Donna Cooper, RN, Elizabeth Greer, RN, Stephanie Yoakum, RNP, Ken Hopper, CVT, Tony Moyeda, CVT, Judy Hildreth, RN, and Cherie Jaynes, RN for their assistance with the clinical portion of this study.

Dr. Krummen has received grant support from the American Heart Association (10 BGIA 3500045) and NIH (HL 83359). Dr. Rappel has received support from the NIH (R01 HL122384). Dr. Narayan has received grant support from the NIH (HL 83359, 103800).

References

1. Kong MH, Fonarow GC, Peterson ED, Curtis AB, Hernandez AF, Sanders GD, Thomas KL, Hayes DL, Al-Khatib SM. Systematic review of the incidence of sudden cardiac death in the united states. *J Am Coll Cardiol.* 2011; 57:794–801. [PubMed: 21310315]
2. Bardy GH, Lee KL, Mark DB, Poole JE, Packer DL, Boineau R, Domanski M, Troutman C, Anderson J, Johnson G, McNulty SE, Clapp-Channing N, Davidson-Ray LD, Fraulo ES, Fishbein DP, Luceri RM, Ip JH. Amiodarone or an implantable cardioverter-defibrillator for congestive heart failure. *N Engl J Med.* 2005; 352:225–237. [PubMed: 15659722]
3. Epstein AE, Dimarco JP, Ellenbogen KA, Estes NA 3rd, Freedman RA, Gettes LS, Gillinov AM, Gregoratos G, Hammill SC, Hayes DL, Hlatky MA, Newby LK, Page RL, Schoenfeld MH, Silka MJ, Stevenson LW, Sweeney MO. *Acc/aha/hrs 2008 guidelines for device-based therapy of cardiac rhythm abnormalities: Executive summary. Heart Rhythm.* 2008; 5:934–955. [PubMed: 18534377]
4. von Kanel R, Baumert J, Kolb C, Cho EY, Ladwig KH. Chronic posttraumatic stress and its predictors in patients living with an implantable cardioverter defibrillator. *J Affect Disord.* 2011; 131:344–352. [PubMed: 21195483]
5. Sweeney MO, Sherfese L, DeGroot PJ, Wathen MS, Wilkoff BL. Differences in effects of electrical therapy type for ventricular arrhythmias on mortality in implantable cardioverter-defibrillator patients. *Heart Rhythm.* 2010; 7:353–360. [PubMed: 20185109]
6. Hohnloser SH, Raeder EA, Podrid PJ, Graboys TB, Lown B. Predictors of antiarrhythmic drug efficacy in patients with malignant ventricular tachyarrhythmias. *Am Heart J.* 1987; 114:1–7. [PubMed: 3604854]
7. Saksena S, Slee A, Waldo AL, Freemantle N, Reynolds M, Rosenberg Y, Rathod S, Grant S, Thomas E, Wyse DG. Cardiovascular outcomes in the affirm trial (atrial fibrillation follow-up investigation of rhythm management). An assessment of individual antiarrhythmic drug therapies compared with rate control with propensity score-matched analyses. *J Am Coll Cardiol.* 2011; 58:1975–1985. [PubMed: 22032709]

8. Haissaguerre M, Extramiana F, Hocini M, Cauchemez B, Jais P, Cabrera JA, Farre J, Leenhardt A, Sanders P, Scavee C, Hsu LF, Weerasooriya R, Shah DC, Frank R, Maury P, Delay M, Garrigue S, Clementy J. Mapping and ablation of ventricular fibrillation associated with long-qt and brugada syndromes. *Circulation*. 2003; 108:925–928. [PubMed: 12925452]
9. Nademane K, Veerakul G, Chandanamatta P, Chaothawe L, Ariyachaipanich A, Jirasitrojankorn K, Likittanasombat K, Bhuripanyo K, Ngarmukos T. Prevention of ventricular fibrillation episodes in brugada syndrome by catheter ablation over the anterior right ventricular outflow tract epicardium. *Circulation*. 2011; 123:1270–1279. [PubMed: 21403098]
10. Knecht S, Sacher F, Wright M, Hocini M, Nogami A, Arentz T, Petit B, Franck R, DeChillou C, Lamaison D, Farre J, Lavergne T, Verbeet T, Nault I, Matsuo S, Leroux L, Weerasooriya R, Cauchemez B, Lellouche N, Derval N, Narayan SM, Jais P, Clementy J, Haissaguerre M. Long-term follow-up of idiopathic ventricular fibrillation ablation: A multicenter study. *J Am Coll Cardiol*. 2009; 54:522–528. [PubMed: 19643313]
11. VanHerendael H, Zado ES, Haqqani H, Tschabrunn CM, Callans DJ, Frankel DS, Lin D, Garcia F, Hutchinson MD, Riley M, Bala R, Dixit S, Yadava M, Marchlinski FE. Catheter ablation of ventricular fibrillation: Importance of left ventricular outflow tract and papillary muscle triggers. *Heart Rhythm*. 2014; 11:566–573. [PubMed: 24398086]
12. Gray RA, Jalife J, Panfilov AV, Baxter WT, Cabo C, Davidenko JM, Pertsov AM. Mechanisms of cardiac fibrillation. *Science*. 1995; 270:1222–1223. author reply 1224–1225. [PubMed: 7502055]
13. Nair K, Umapathy K, Farid T, Masse S, Mueller E, Sivanandan RV, Poku K, Rao V, Nair V, Butany J, Ideker RE, Nanthakumar K. Intramural activation during early human ventricular fibrillation. *Circulation*. 2011; 4:692–703. [PubMed: 21750274]
14. Nash MP, Mourad A, Clayton RH, Sutton PM, Bradley CP, Hayward M, Paterson DJ, Taggart P. Evidence for multiple mechanisms in human ventricular fibrillation. *Circulation*. 2006; 114:536–542. [PubMed: 16880326]
15. Krummen DE, Hayase J, Morris DJ, Ho J, Smetak MR, Clopton P, Rappel WJ, Narayan SM. Rotor stability separates sustained ventricular fibrillation from self-terminating episodes in humans. *J Am Coll Cardiol*. 2014; 63:2712–2721. [PubMed: 24794115]
16. Pak HN, Kim GI, Lim HE, Fang YH, Choi JI, Kim JS, Hwang C, Kim YH. Both Purkinje cells and left ventricular posteroseptal reentry contribute to the maintenance of ventricular fibrillation in open-chest dogs and swine: Effects of catheter ablation and the ventricular cut-and-sew operation. *Circulation J*. 2008; 72:1185–1192.
17. Narayan SM, Krummen DE, Shivkumar K, Clopton P, Rappel WJ, Miller JM. Treatment of atrial fibrillation by the ablation of localized sources: Confirm (conventional ablation for atrial fibrillation with or without focal impulse and rotor modulation) trial. *J Am Coll Cardiol*. 2012; 60:628–636. [PubMed: 22818076]
18. Cassidy DM, Vassallo JA, Marchlinski FE, Buxton AE, Untereker WJ, Josephson ME. Endocardial mapping in humans in sinus rhythm with normal left ventricles: Activation patterns and characteristics of electrograms. *Circulation*. 1984; 70:37–42. [PubMed: 6723010]
19. Vassallo JA, Cassidy DM, Miller JM, Buxton AE, Marchlinski FE, Josephson ME. Left ventricular endocardial activation during right ventricular pacing: Effect of underlying heart disease. *J Am Coll Cardiol*. 1986; 7:1228–1233. [PubMed: 3711479]
20. Cao JM, Qu Z, Kim YH, Wu TJ, Garfinkel A, Weiss JN, Karagueuzian HS, Chen PS. Spatiotemporal heterogeneity in the induction of ventricular fibrillation by rapid pacing: Importance of cardiac restitution properties. *Circulation Res*. 1999; 84:1318–1331. [PubMed: 10364570]
21. Swerdlow CD, Russo AM, Degroot PJ. The dilemma of ICD implant testing. *Pacing Clin Electrophysiol*. 2007; 30:675–700. [PubMed: 17461879]
22. Narayan SM, Krummen DE, Rappel WJ. Clinical mapping approach to diagnose electrical rotors and focal impulse sources for human atrial fibrillation. *J Cardiovasc Electrophysiol*. 2012; 23:447–454. [PubMed: 22537106]
23. Umapathy K, Nair K, Masse S, Krishnan S, Rogers J, Nash MP, Nanthakumar K. Phase mapping of cardiac fibrillation. *Circulation*. 2010; 3:105–114. [PubMed: 20160178]

24. Narayan SM, Franz MR, Lalani G, Kim J, Sastry A. T-wave alternans, restitution of human action potential duration, and outcome. *J Am Coll Cardiol.* 2007; 50:2385–2392. [PubMed: 18154963]
25. Narayan SM, Bayer JD, Lalani G, Trayanova NA. Action potential dynamics explain arrhythmic vulnerability in human heart failure: A clinical and modeling study implicating abnormal calcium handling. *J Am Coll Cardiol.* 2008; 52:1782–1792. [PubMed: 19022157]
26. Gray RA, Pertsov AM, Jalife J. Spatial and temporal organization during cardiac fibrillation. *Nature.* 1998; 392:75–78. [PubMed: 9510249]
27. Haissaguerre M, Shoda M, Jais P, Nogami A, Shah DC, Kautzner J, Arentz T, Kalushe D, Lamaison D, Griffith M, Cruz F, de Paola A, Gaita F, Hocini M, Garrigue S, Macle L, Weerasooriya R, Clementy J. Mapping and ablation of idiopathic ventricular fibrillation. *Circulation.* 2002; 106:962–967. [PubMed: 12186801]
28. Davidenko JM, Kent PF, Chialvo DR, Michaels DC, Jalife J. Sustained vortex-like waves in normal isolated ventricular muscle. *Proc Natl Acad Sci USA.* 1990; 87:8785–8789. [PubMed: 2247448]
29. Zaitsev AV, Guha PK, Sarmast F, Kolli A, Berenfeld O, Pertsov AM, de Groot JR, Coronel R, Jalife J. Wavebreak formation during ventricular fibrillation in the isolated, regionally ischemic pig heart. *Circulation Res.* 2003; 92:546–553. [PubMed: 12600877]
30. Kim YH, Xie F, Yashima M, Wu TJ, Valderrabano M, Lee MH, Ohara T, Voroshilovsky O, Doshi RN, Fishbein MC, Qu Z, Garfinkel A, Weiss JN, Karagueuzian HS, Chen PS. Role of papillary muscle in the generation and maintenance of reentry during ventricular tachycardia and fibrillation in isolated swine right ventricle. *Circulation.* 1999; 100:1450–1459. [PubMed: 10500048]
31. Miller JM, Kowal RC, Swarup V, Daubert JP, Daoud EG, Day JD, Ellenbogen KA, Hummel JD, Baykaner T, Krummen DE, Narayan SM, Reddy VY, Shivkumar K, Steinberg JS, Wheelan KR. Initial independent outcomes from focal impulse and rotor modulation ablation for atrial fibrillation: Multicenter firm registry. *J Cardiovasc Electrophysiol.* 2014; 25:921–929. [PubMed: 24948520]
32. Narayan SM, Baykaner T, Clopton P, Schricker A, Lalani GG, Krummen DE, Shivkumar K, Miller JM. Ablation of rotor and focal sources reduces late recurrence of atrial fibrillation compared with trigger ablation alone: Extended follow-up of the confirm trial (conventional ablation for atrial fibrillation with or without focal impulse and rotor modulation). *J Am Coll Cardiol.* 2014; 63:1761–1768. [PubMed: 24632280]
33. Zima E, Gergely M, Soos P, Geller LA, Nemes A, Acsady G, Merkely B. The effect of induction method on defibrillation threshold and ventricular fibrillation cycle length. *J Cardiovasc Electrophysiol.* 2006; 17:377–381. [PubMed: 16643358]
34. Mandapati R, Asano Y, Baxter WT, Gray R, Davidenko J, Jalife J. Quantification of effects of global ischemia on dynamics of ventricular fibrillation in isolated rabbit heart. *Circulation.* 1998; 98:1688–1696. [PubMed: 9778336]
35. Wellner M, Berenfeld O, Jalife J, Pertsov AM. Minimal principle for rotor filaments. *Proc Natl Acad Sci USA.* 2002; 99:8015–8018. [PubMed: 12048234]
36. Rappel WJ, Narayan SM. Theoretical considerations for mapping activation in human cardiac fibrillation. *Chaos.* 2013; 23:023113. [PubMed: 23822478]
37. Hayase J, Tung R, Narayan SM, Krummen DE. A case of a human ventricular fibrillation rotor localized to ablation sites for scar-mediated monomorphic ventricular tachycardia. *Heart Rhythm.* 2013; 10:1913–1916. [PubMed: 23911894]
38. Kamimura T, Sakamoto H, Misumi K, Hirakawa A, Shimizu R, Akuzawa M, Miyahara K. Left ventricular wall thickness in normal mongrel dogs. *J Vet Med Sci.* 1993; 55:591–594. [PubMed: 8399738]
39. Sultan A, Luker J, Hoffmann B, Servatius H, Aydin A, Nuhric J, Akbulak O, Schreiber D, Schaffer B, Rostock T, Willems S, Steven D. Necessity of epicardial ablation for ventricular tachycardia after sequential endocardial approach. *Int J Cardiol.* 2015; 182:56–61. [PubMed: 25576719]

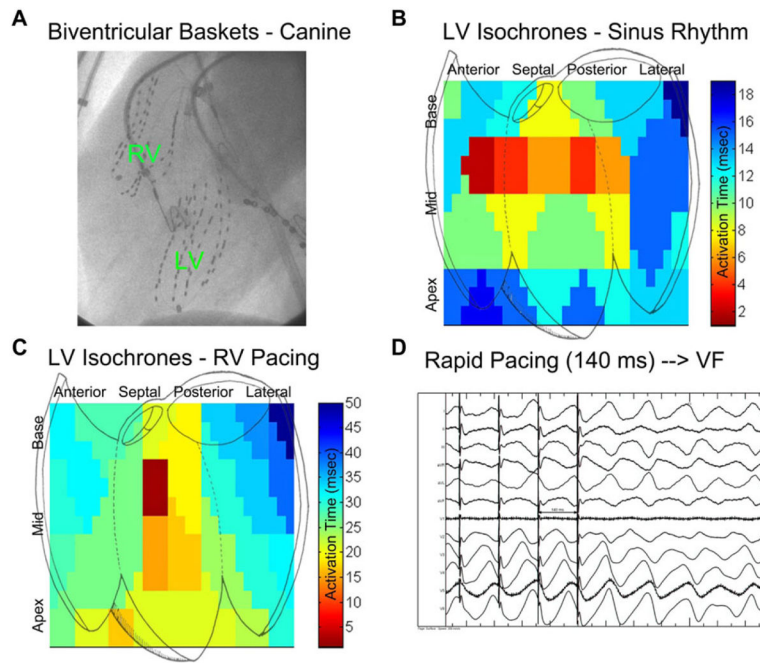


Figure 1.

Canine electrophysiology study and VF induction. A: Left anterior oblique cine showing biventricular baskets (left ventricular basket inserted retrograde across the aortic valve, RV basket via the inferior vena cava). B: Isochronal analysis of left ventricular activation during sinus rhythm is shown. Note activation from anterior and posterior fascicles (red locations). C: Isochronal analysis during rapid right ventricular pacing (cycle length 200 milliseconds). The location of septal breakthrough is indicated by deep red. No rotational artifact is noted. D: Induction of VF via rapid RV pacing at a CL of 140 milliseconds in canine 7.

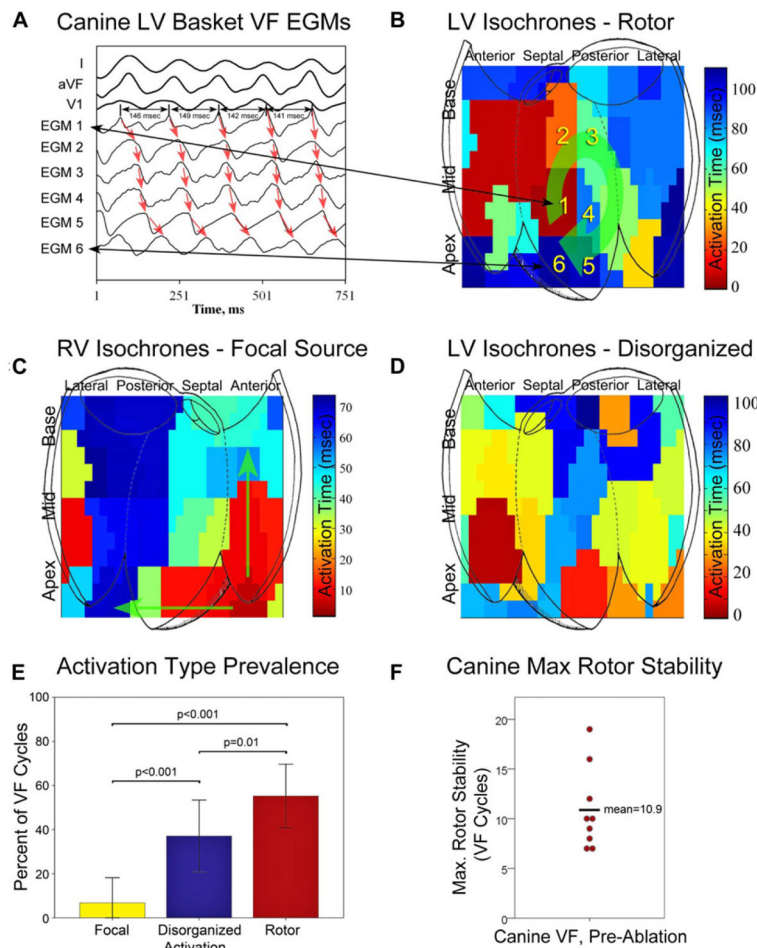


Figure 2. Canine VF activation types, prevalence, and maximum rotor stability. A: LV basket electrograms near rotor core (average cycle length for EGM1 in this figure is 145 milliseconds). B: LV isochronal analysis shows mid-posteroseptal LV rotor (green arrow) with a cycle length of 145 milliseconds (canine 7). Numbers indicate corresponding electrograms in 2A. C: An example of right ventricular focal activation (green arrows) during VF (canine 6). D: Disorganized activity during VF (canine 7). E: Preablation canine VF activation patterns are shown; VF was predominantly characterized by rotors (56 ± 14% of VF cycles), with smaller proportions of disorganized activity (35 ± 15%), and focal activation (7 ± 11%, P values as shown). F: Maximum canine rotor stability is plotted for each subject; average 10.9 ± 4.1 rotations.

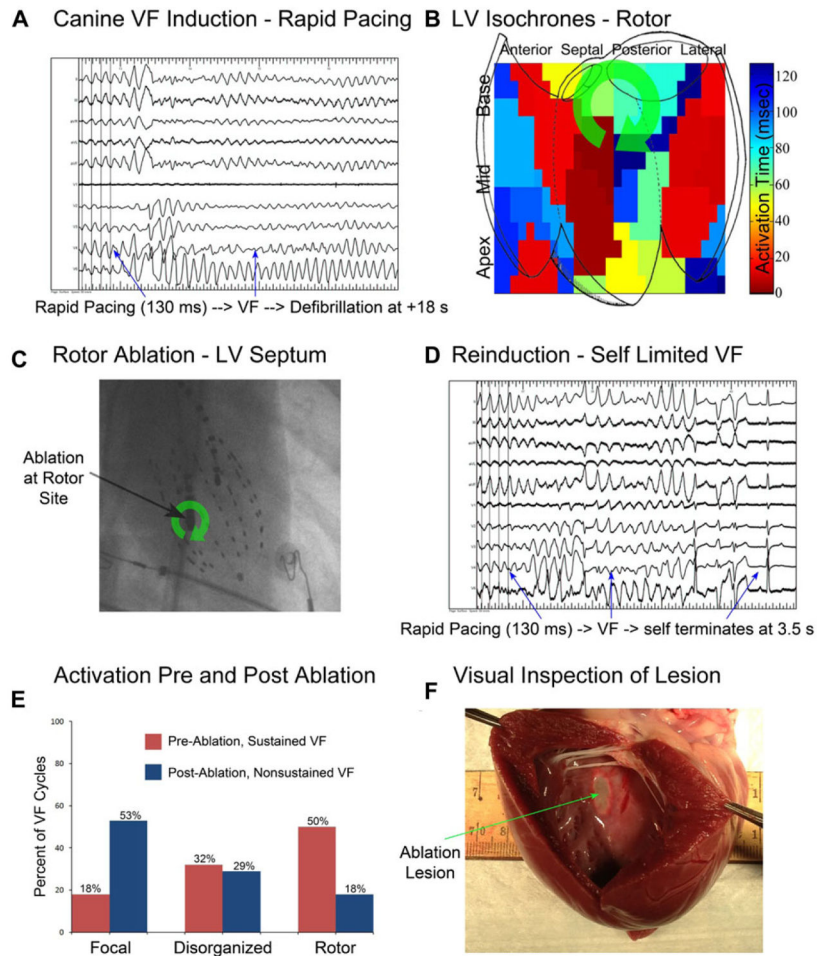


Figure 3. Canine rotor substrate ablation prevents sustained VF and reduces rotor prevalence. A: Rapid pacing at 130 milliseconds induces sustained VF, requiring defibrillation. B: Isochronal analysis shows mid postero-septal LV rotor. C: Anteroposterior cine, showing LV ablation catheter and LV basket catheter, during which targeted rotor substrate ablation was performed. Ablation delivered 8 minutes of RF energy to rotor substrate site (green arrow). D: Following ablation, 5 seconds of rapid pacing at 130 milliseconds induces self-limited VF; more rapid pacing resulted in 2:1 block. E: Comparison of activation type prevalence, pre and postablation in this animal. Note the decrease in rotor prevalence following successful ablation from 50% of VF cycles to 18% of VF cycles. F: Visual inspection of targeted substrate ablation site shows ablated area (green arrow to lesion) measuring 2.2 cm².

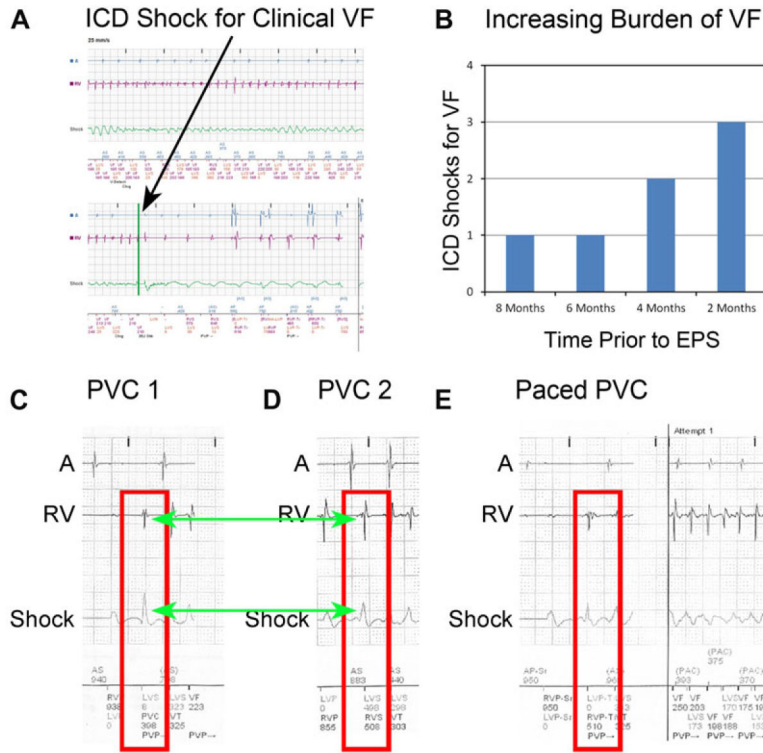


Figure 4. Clinical VF, burden, and polymorphic triggers. A: Preablation ICD interrogation shows clinical VF, requiring defibrillation. The patient had a total of 7 episodes of VF in the 8 months prior to ablation. B: Plot of ICD shocks preceding VF rotor substrate site ablation, showing an increasing burden despite sotalol therapy. C and D: Two distinct, nonpaced PVC morphologies initiating VF. E: PVC initiating VF with an origin closer to RV lead which elicited triggered LV pacing.

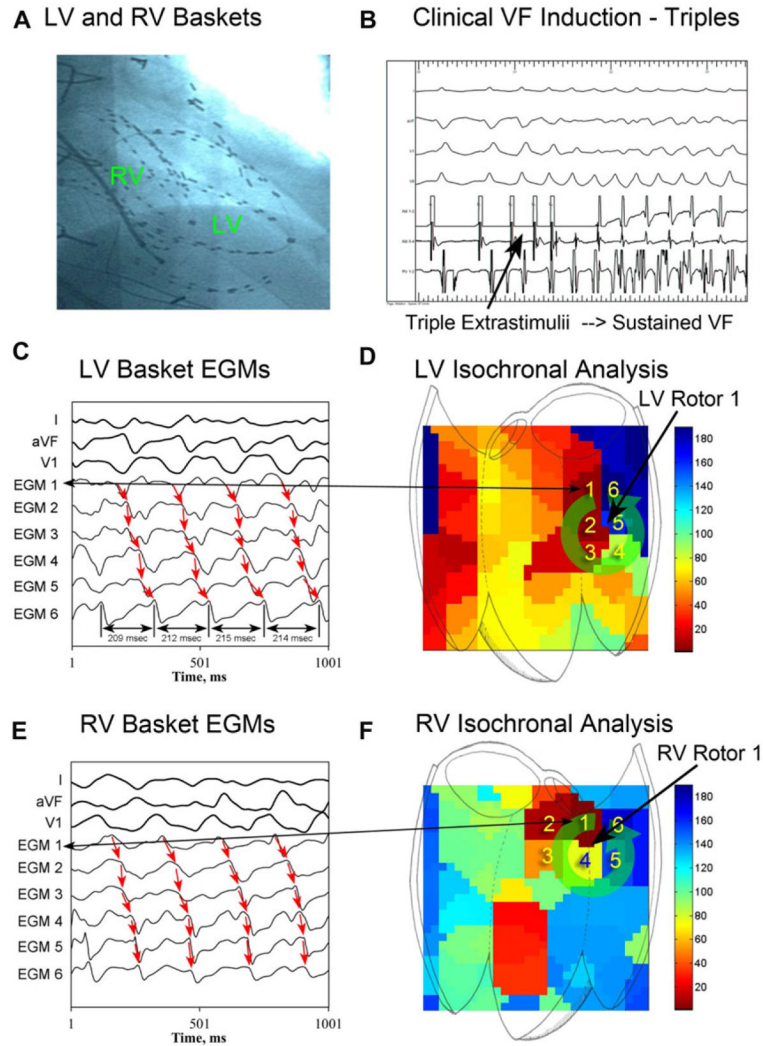


Figure 5. Biventricular human VF mapping. A: Right anterior oblique cine showing biventricular basket catheters during VF mapping. B: Triple extrastimuli at 500–330–220–180 induces sustained VF, requiring defibrillation. C: LV basket electrograms (EGMs) surrounding LV rotor phase singularity during VF. Cycle lengths from EGM 6 (average CL 213 milliseconds) are shown. D: LV isochronal analysis shows counterclockwise LV rotor 1. Numbers 1–6 indicate corresponding electrograms from 6C. E: RV basket EGMs during VF surrounding rotor phase singularity showing sequential activation. F: Isochronal plot showing RV rotor 1. Numbers 1–6 indicate corresponding electrograms from 6E.

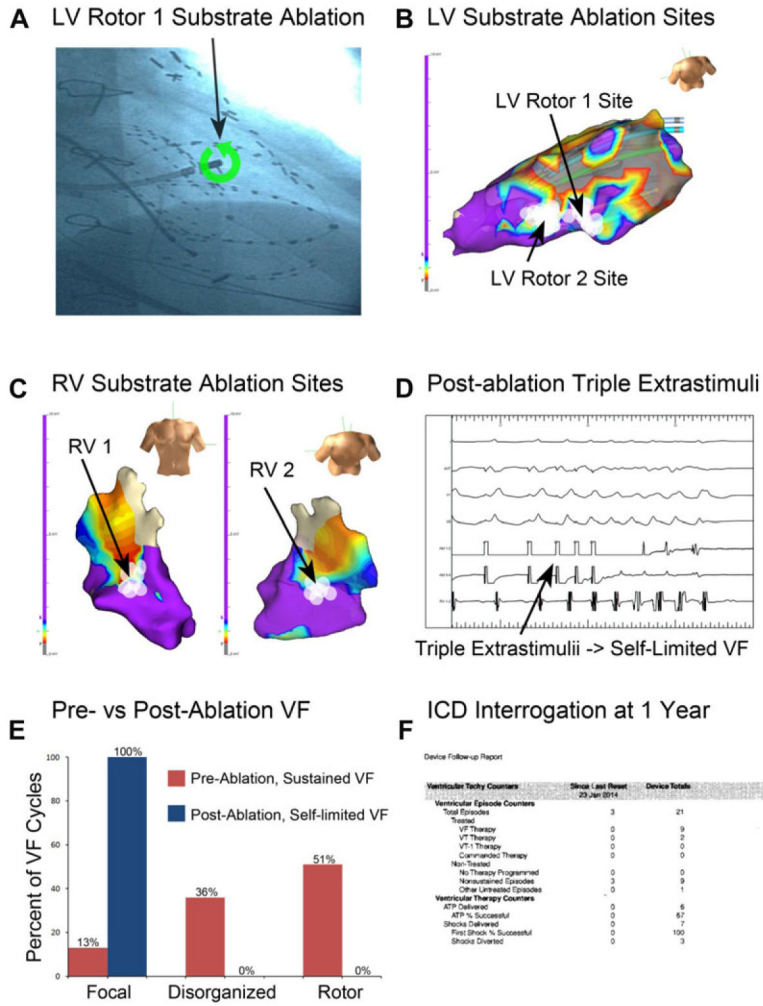


Figure 6. VF rotor substrate site ablation and follow-up. A: Right anterior oblique cine of showing the ablation catheter positioned at LV rotor site 1. B: LV voltage map and LV rotor site 1 and 2 ablation lesions (white circles), located at borderzone tissue (red to blue voltage areas). C: RV voltage map showing ablation lesions for RV rotor site 1 (left) and site 2 (right). D: Following rotor substrate ablation, triple extrastimuli induces self-limited VF (at 500–320–220–190, lasting <2 seconds), but not sustained VF. E: Ablation decreased the VF rotor prevalence from 51% preablation to 0% postablation. F: ICD interrogation at 1 year shows no sustained or treated VF events since ablation, without antiarrhythmic drug therapy.

TABLE 1

Canine VF Study Summary

Study ID	Sex	Age (y)	Weight (kg)	VF Induction Threshold (milliseconds)	VF CL (milliseconds)	Sustained VF Inducible Postablation
Canine 1	F	7.2	29.5	150	110	No
Canine 2	F	3.5	18.1	150	124	No
Canine 3	F	3.6	18.1	160	138	No
Canine 4	F	3.7	19.9	180	106	No
Canine 5	F	0.7	17.2	110	114	No
Canine 6	F	2.5	20.0	160	127	Yes
Canine 7	F	1.0	20.5	140	110	No
Canine 8	M	0.6	18.2	160	144	Yes* (*Nonsustained Only, Fig. 4)
Canine 9	M	0.6	20.5	140	118	Yes